AAG2020

Advances in Architectural Geometry 2020
Ecole des Ponts, Univ. Gustave Eiffel
Champs-sur-Marne, France

The Canopy Pavilion

A lightweight shading structure using a deployable auxetic linkage membrane

Florin Isvoranu[1] Tian Chen[1] Etienne Bouleau[2] Arthur Blanc[1] Dieter Dietz[1]
Mark Pauly[1, *]

[1] EPFL [2] Lüchinger+Meyer
[*] Corresponding author e-mail: mark.pauly@epfl.ch

Abstract

We present the *Canopy Pavilion*, a lightweight shading structure for a social gathering space. The shading surface is realized as a tensioned auxetic linkage membrane, composed of two double-curved anticlastic layers separated by a compression pole. The membrane is assembled flat on the ground from laser-cut hexagonal aluminium panels, and is subsequently mounted on a circular support frame. Tensioning then deploys the surface to its desired target shape. We apply numerical optimization to form-find the equilibrium shape of the tensioned membrane. The geometry of each individual linkage panel is further adapted to reduce material usage, while maximizing the main function of the structure, to provide shading. Our material system offers a number of distinct advantages. Individual panels can be cut from standard sheet material, all connections between panels are identical, the surfaces can be assembled on the ground and deployed easily to their double-curved shape. The pavilion is a first demonstrator for a novel lightweight construction system at architectural scale that has potential applications in facades, roofs, or support structures.

Keywords: auxetic structures, deployable membrane, form finding, computational design, numerical optimization

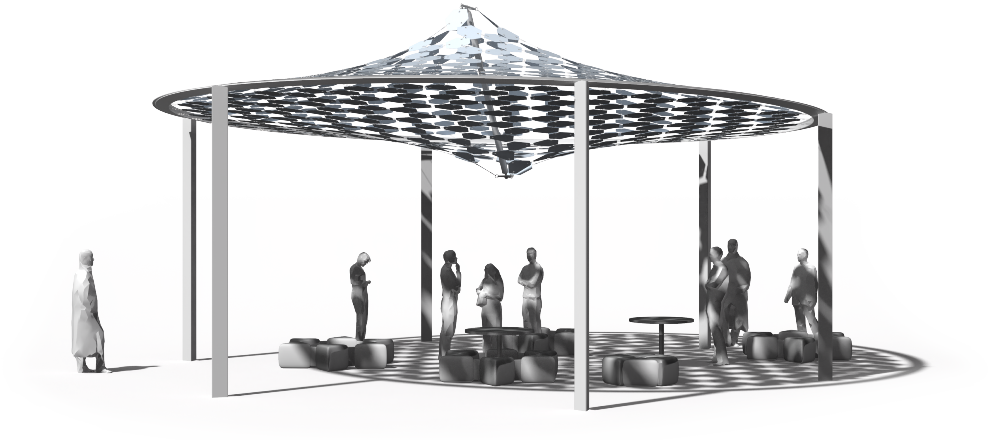

Figure 1: The Canopy Pavilion. A lightweight shading structure using a deployable auxetic linkage membrane.

1 Introduction

Place Cosandey, a recently re-developed large outdoor space at the École Polytechnique Fédérale de Lausanne (EPFL), combines various social functions at the heart of a lively campus. A barbecue grill and its surrounding seating area has become a popular gathering space for students, staff, and visitors. Trees have only recently been planted, so they do not yet provide enough protective shade for a pleasant experience during the hot hours of summer. The Canopy Pavilion is designed to address this problem (see Figure 1).

The main shading surface is a two-layered tensioned membrane mounted on a circular support frame. The membrane is composed of planar hexagonal aluminium panels that are joined with wire connectors. This linkage structure can be assembled on the ground and subsequently tensioned to assume its programmed double-curved shape. It thus combines the possibilities of an expressive design with efficient fabrication and construction, while offering excellent structural performance and durability. To facilitate a more detailed study of the pavilion, we will publish the form-finding code, the structural analysis models, geometric data, VR environment, and photos and videos of the construction process and final pavilion at `canopy.epfl.ch`.

Overview. In Section 2 we explain the project context and motivate the main design decisions. The core underlying membrane structure is based on an auxetic material system that facilitates simple CNC-based fabrication, efficient assembly, and rapid deployment. We review in Section 3 the geometric principles of linkage-based auxetics. To design a structurally efficient membrane, we adapt the geometry

Figure 2: Left: Connection detail of the cooling tower of Schmehausen, see Schlaich and Bergermann (2004). Middle: connection detail of the Nest Hilo prototype, see Mendez Echenagucia et al. (2019). Right: Early prototype of connection detail of the Canopy Pavilion.

of the plate elements using a form-finding optimization as discussed in Section 4. We further refine the plate geometry to control the key performative aspect of the pavilion, to provide ample shade with minimal material usage. In Section 5 we show how a parametric model can be explored in a virtual reality environment to interactively design the shading experience. We perform a detailed structural analysis in Section 6 to inform the dimensioning of membrane elements and ensure compliance with building codes. Section 7 discusses fabrication- and construction-related issues.

Related Work. Early tensioned structure projects were developed using steel ropes, mostly oriented in two directions as in the Munich Stadium by Frei Otto, and occasionally in three directions like the Cooling Tower Schmehausen by Schlaich, see Schlaich and Bergermann (2004). The use of materials such as membranes appeared as early as the 1980s, for example in the Montreal stadium, whose natural flexibility facilitates tensioning. Some more recent projects use non-extensible materials, such as the facade of the Kukje Art Centre in Seoul, which is made with a metal ring mesh, see Kock et al. (2012). The majority of cable nets use the standard detail used in the Cooling tower allowing several layers of cable pairs to cross each other. Recently the Nest Hilo roof project developed a different connection with small pieces of cables each one different from each other to form a free-shape surface as discussed in Mendez Echenagucia et al. (2019).

The use of flat aluminium panels to realize negative curvature tensioned surfaces, as the sculpture Tour de Force designed by Marc Fornes (2016), implies a twist at the connection of two plates. In the Canopy Pavilion, this twist is facilitated by using a standardized connection made of stainless-steel wire. The double-curved surface is programmed by optimizing the shape of the aluminium panels in the auxetic linkage. Spatially graded auxetic linkage structures have recently been proposed architectural research as a means to design freeform facades Konaković-Luković et al. (2018) or concrete formwork Friedrich et al. (2018). We refer to these papers for a broader discussion.

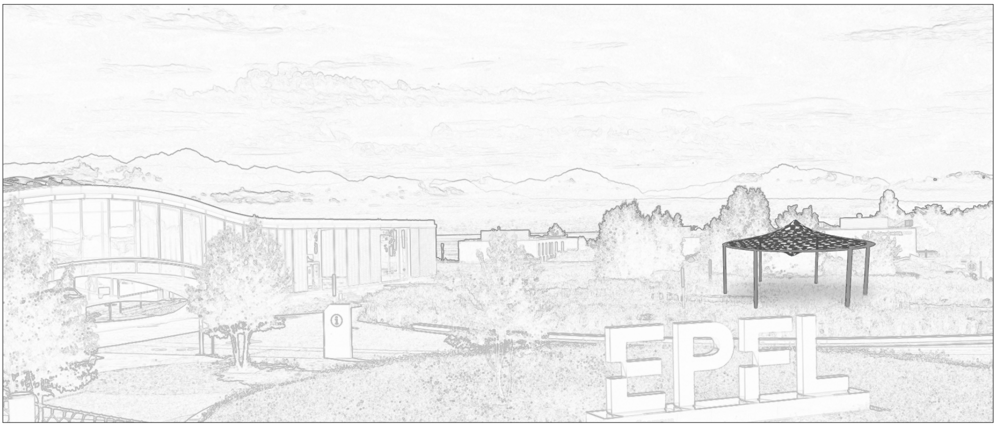

Figure 3: Place Cosandey is the central outdoor gathering space at EPFL.

2 Project Context and Main Design Decisions

The Canopy Pavilion is embedded in a large open space on EPFL campus as illustrated in Figure 3. One dominant design theme of this space is the circle, which motivates our use of a circular ring for the membrane boundary frame. The circle provides excellent structural behavior under contractive forces required for tensioning the membrane. The circular frame of inner radius of 10 meters is mounted on six columns at an average height of 4 meters to obtain a minimum of 3 meters clearance under the structure.

The key technical element of the pavilion is a double-layer membrane realized as an auxetic linkage structure mounted on the circular frame. The top and bottom layers are composed of 347 and 281 variably-sized aluminium panels, respectively. The different number of panels for the top and bottom surface is motivated by the total area of the equivalent smooth surface and the amount of curvature and plate-to-plate twist that needs to be distributed over the respective number of plates. Neighboring panels are connected with thin wires and form an ensemble of seemingly floating shading elements to create a shading experience reminiscent of layers of tree leaves. The two layers are linked by a compression pole that acts as an important structural element, but also leads to a graded spatial separation between the layers, creating a dynamic shadow pattern on the ground as the sun transitions across the sky (see also Figure 5C). The form-found shape of the membrane is inspired by the silhouettes of the mountains on the horizon when seen from the center of the square. We accentuate this connection by inclining the ring by 4 degrees towards NNW at azimuth 343 degrees.

To emphasize the importance of the sun position for the shading performance, the orientation of the compression pole is chosen to match the direction of sunlight at the solar noon of the summer solstice for the precise location of the pavilion. This direction of 66.92 degrees towards the South corresponds to the time when the shadow cast by a vertical pole is smallest, hence thermal intensity of sunlight is

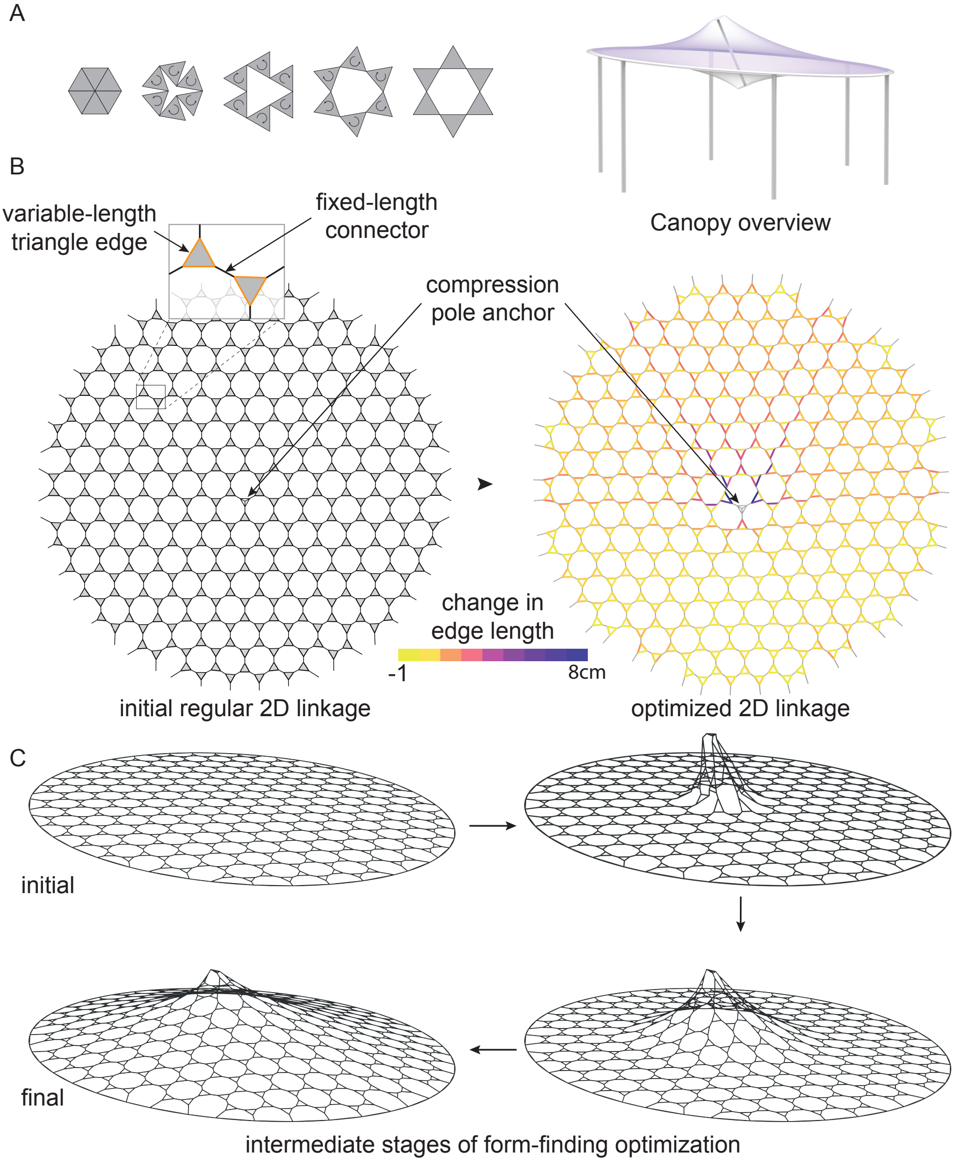

Figure 4: The auxetic membrane. A: Geometric principle: The triangle linkage expands uniformly until fully opened by allowing triangles to rotate around vertex joints. B: Optimization of the top layer: Starting from an initial uniform pattern (left), our form-finding optimization determines the shape of each triangle (right) such that the deployed membrane matches the design target. Color-coding indicates the change in length of triangle edges from the initial to final optimized shape. The linkage is stretched out in the plane for better visualization. C: Several stages of the iterative form-finding optimization.

at its peak.

Detailing is deliberately kept minimal to highlight the geometric simplicity of the linkage structure despite the complex freeform surface that it assumes. Steel is chosen for the support frame and connectors, while panels are cut from aluminium sheets, in order to maximize durability and minimize maintenance often required for fabric-based shading structures. The connection between adjacent panels is realized by a wire loop to allow for the necessary rotation and twisting of panels. Importantly, the connector wires have a fixed length of 27.3 cm to ensure that all connections are identical, which simplifies fabrication and assembly.

3 Triaxial Auxetic Linkage

The canopy membrane surface is based on a 2D auxetic material system (Figure 4). The term *auxetic* refers to the uncommon deformation behavior with negative Poisson's ratio; when stretched, the material expands in the direction perpendicular to the applied force. The basic geometric construction in our design connects rigid triangles at their vertices to form a triaxial linkage (Kagome pattern), see Konaković et al. (2016) for details. The plates are later enlarged towards a hexagonal shape to increase their shading capacity. The structurally relevant geometry, however, are still the triangles defined by the topology of the linkage structure.

When an expansive force is applied, the triangles rotate around the vertex hinge joints to increase the overall surface area by enlarging the hexagonal openings as illustrated in Figure 4A. To obtain a structurally stable membrane in static equilibrium under tension, we require the linkage to be maximally expanded everywhere. As a consequence, all hexagonal openings are fully extended. We obtain a curved surface from the initially flat assembly state by varying the relative expansion, as explained in Konaković-Luković et al. (2018); Friedrich et al. (2018). This can be achieved by scaling the triangles of the linkage non-uniformly across the surface.

This behavior is well-known in differential geometry for continuous conformal deformations and formalized in the Yamabe equation that relates the Laplacian of the logarithmic length expansion factor to the Gaussian curvature of the surface. For a detailed discussion about the mathematical background we refer to Konaković-Luković et al. (2018), where an inverse design algorithm is proposed based on a conformal flattening of the desired design surface. Our approach differs in that we apply a direct form finding optimization by minimizing an elastic membrane energy as detailed below.

4 Form-Finding

The geometric shape of the membrane is determined by an optimization-based form-finding process that aims at maximizing structural performance while meeting the functional and aesthetic design constraints. The two layers of the shading membrane have a fixed outer boundary defined by the circular support frame. In addition, each layer is attached to opposite ends of the compression pole (see Figure 4), which defines additional (variable) boundary constraints. To control the design, we fix the length and orientation of the pole, but let its position vary during the optimization. The goal is then to find an equilibrium state where all membrane elements experience tensile forces only, so that no compression or bending forces

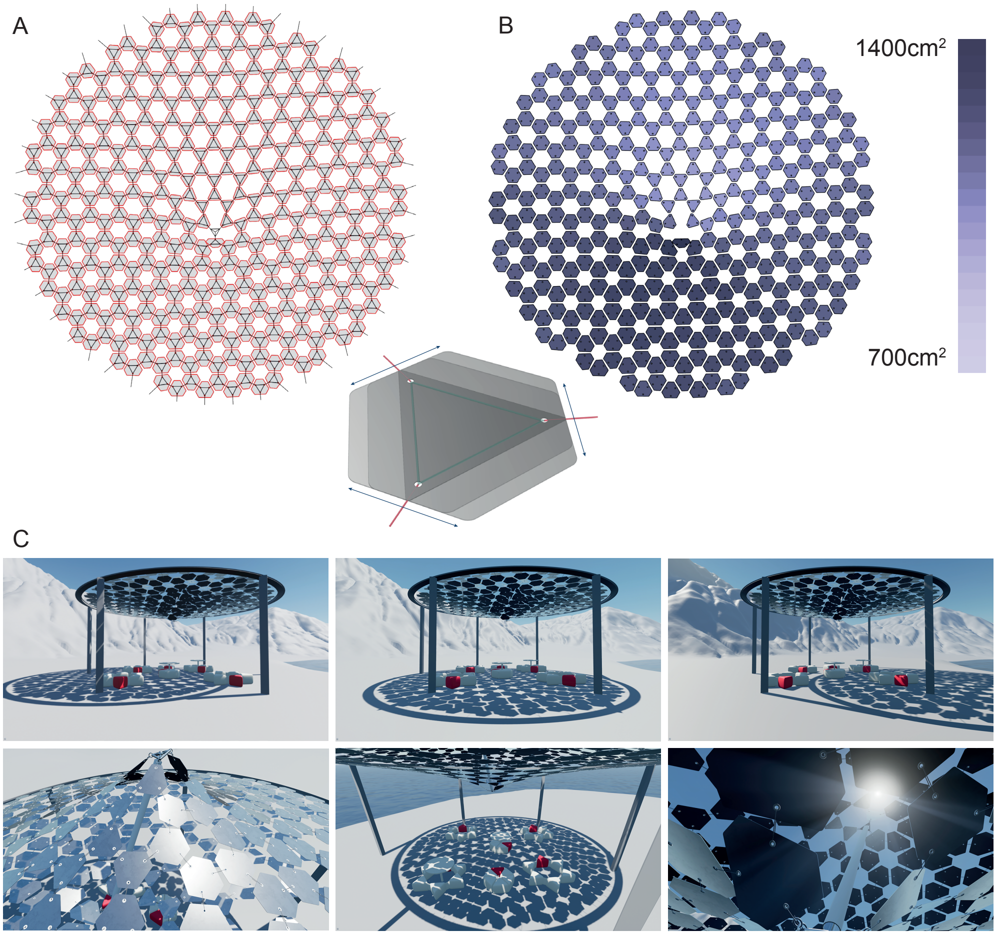

Figure 5: Shadowing. A: The structural triangles (black lines) of the optimized 2D linkage (here only shown for the top layer) are enlarged to hexagonal shapes (red lines) based on their relative shading capacity. B: Color-coding of the resulting panel areas. Note how the entire membrane layer can still be assembled on the ground without overlap between panels. C: Screenshots of our virtual reality simulation to explore shading parameters.

are acting on the plates or wire connectors. The connecting pole should be in pure compression without any torsion to counteract the tensile forces in the structure.

We initialize each membrane layer with a planar regular triaxial pattern (Kagome lattice). To account for the physical connections in the form-found geometry and make sure we use the correct force path for the FEA modeling, we shrink the triangles and connect them with an edge of fixed length representing the fixed wire loop connectors (see Figure 4). Each triangle edge is modeled as a tensile spring. To provide design control, we allow the user to specify different spring rest lengths at the top and bottom layer. In this way, we can slightly flatten the lower layer to avoid having its lowest point approach the ground too much. The slight flattening of the lower membrane enables us to shorten the columns that support the structure while keeping the minimum clearance of 3 meters.

Wire connections to the boundary ring can freely slide along the circle during the optimization to reduce stress. The attachment locations of the compression pole to each layer is manually selected. A fixed-length and orientation constraint is used to define the behavior of the compression pole that retains free translational degrees of freedom. The optimization is based on the projective dynamics method of Bouaziz et al. (2014); Deuss et al. (2015) implemented in Kangaroo 2.

Various settings of the design parameters have been explored interactively, namely: the plate-to-plate gap, the plate shape and expanded size, and the plate-to-plate connection length. We chose a length of 2.6 meters for the compression pole and set its orientation to an inclination of 66.92 degrees towards South corresponding to the solar noon at the summer solstice. We verify flat-assemblability by ensuring that the lengths of the longest and shortest triangle edge do not exceed a ratio of two, the limit of expansion for the triaxial linkage.

5 Shading

An important design goal of the Canopy Pavilion is to achieve maximal shading performance with low material usage. We therefore adapt the sizing of elements according to their shadowing characteristics. The triangles of the linkage can be enlarged into hexagons as illustrated in Figure 5, without affecting their main structural properties as the connection holes remain unchanged.

Essentially, the orientation of a panel with respect to the incoming sunlight direction determines its relative shading capacity, defined as the area of the cast shadow on the ground relative to the area of the panel. Naturally, this shading capacity changes as the sun moves across the sky. We simplify the computation by choosing a single sun direction for plate size adaptation corresponding to the average sun vector from day 141 to 232 of the year, between 10:00AM and 17:00PM. The average sun vector for the chosen period has a 62deg153min elevation and 191deg414min azimuth. We calculate the angle between this direction and the normal vector of each panel, normalize all angles to a range of $[0, 1]$ and clamp these values to an interval of $[0.3, 0.85]$ to balance panel sizes more evenly. Finally we laterally stretch the edges of the hexagons as illustrated in Figure 5A in proportion to this value, using a global scale factor λ to control the overall shading capacity. As the orientation of elements varies smoothly across the surface, the sizing also adapts continuously, leading to a visually pleasing smooth gradation of element sizes. In addition, we average the edge lengths of adjacent panels to ensure a smooth transition across the connections.

The global parameter λ has been adapted interactively using a virtual reality (VR) environment illustrated in Figure 5C. The top row images show the evolution of the shadow pattern during the course of a day, the bottom row highlights some additional views of an interactive exploration. The VR setup has been instrumental in assessing perceptual aspects of the design that are difficult to formalize or model analytically. In particular, the visual experience of light and shadow when moving under the pavilion, the overall shading levels, and the general quality of light can

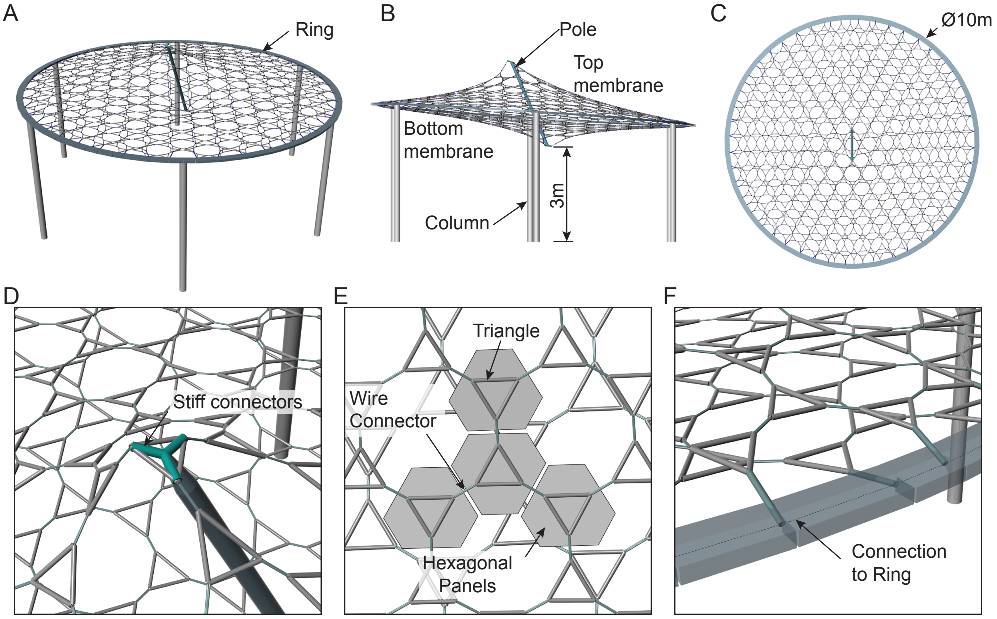

Figure 6: Setup of the simplified FE model. A-C: Different views of the beam based FE model. D-F: Detailed schematic of the different components.

best be appreciated in a VR. The interested reader is invited to explore the design by downloading the VR data at `canopy.epfl.ch`. The final selected value of λ leads to an overall shadowing of 80% of the total boundary circle area.

6 Structural Analysis

The Canopy Pavilion is a double-layer tensioned circular surface with a stiff rod in the center (the compression pole), attached to an annular edge ring in compression. Both layers work together: the tensioned bottom layer carries the dead load and the snow load, while the tensioned top layer carries the uplift wind load. Ordinarily, each layer stabilizes the other creating a stiff structure against uplift and downward loading. For both service and ultimate state, we must ensure the structure does not deform excessively, and does not reach yield stress. The characteristic value of the snow load is a downward pressure of $s_\mathrm{k} = 0.9\,\mathrm{kN\,m^{-2}}$, the accumulation of ice in between the two layers is not taken into account in this study. Directly exposed to the sun, the aluminium undergoes a temperature variation and a thermal expansion that affect the tension in both layers and consequently the global deflection. We consider a temperature range of $-20\,°\mathrm{C}$ to $10\,°\mathrm{C}$ in winter and $10\,°\mathrm{C}$ to $40\,°\mathrm{C}$ during summer, which means a maximum temperature variation of $30\,°\mathrm{C}$ is applied on the steel and aluminium elements. The magnitude of the wind loads we consider are an interpretation from the case study specified in the Swiss building codes with the main wind direction observed on site (North East – South West). The characteristic value of wind is $q_{\mathrm{p}0} = 0.9\,\mathrm{kN\,m^{-2}}$, which gives a design pressure of $q_\mathrm{p} = 1.15\,\mathrm{kN\,m^{-2}}$. In absence of a detailed CFD analysis, the uplift is applied as a static load that is in line with the analytical approach of the building codes. In addition, accidental loads are analyzed: 1) an overextension of the center pole during deployment, 2) an accidental mass of 2kN on one of the hexagonal panels or 3) at the base of the pole. Two separate simulations are conducted, the first using a simplified global Finite Element model of the structure, the second using a volumetric model of one hexagonal panel with connectors.

Geometrical non-linearities are considered for both simulations. For the first model, all structural elements are considered as beams of different cross section area (Fig. 6A-C). The superstructure consisting of the membranes and the pole are connected to the ring beam, which in turn is supported on six equally spaced columns. Fixed boundary conditions (i.e. no translation or rotation) are applied to the base of the columns. The pole is fixed to the center of the top and the bottom hexagonal panels (Fig. 6D). We simplify the computation by representing each panel by three beams forming a triangle, with neighboring panels connected by wire loops (Fig. 6E). The outer ring is modeled as having a flat rectangular profile, the connecting elements extending to this outer ring (Fig. 6F). The outer ring rests on the columns, transferring both torques and forces. Linear elasticity is assumed for both steel ($E_s = 210\,\mathrm{GPa}, \rho = 7850\,\mathrm{kg\,m^{-3}}$) and aluminium ($E_s = 70\,\mathrm{GPa}, \rho = 2700\,\mathrm{kg\,m^{-3}}$). The aluminium panels have a rough finish, the grade is a EN AW-6082 T6, with an elastic resistance $R_{\mathrm{p,min}} = 260\,\mathrm{MPa}$. The coefficient of thermal expansion is set at $13 \times 10^{-6}\,{}^{\circ}\mathrm{C}^{-1}$ for steel and $23.1 \times 10^{-6}\,{}^{\circ}\mathrm{C}^{-1}$ for aluminium. Moment transfer is restricted to connections between the ring and the columns, and between the pole and hexagonal panels at the top and bottom.

First gravity is imposed, then the superimposed load cases are considered sequentially in addition to gravity. The snow and wind loads are converted from pressures to line loads on the triangles based on the projected area to the respective planes. For the thermal loads, the ambient temperature is set instantaneously, and steady states are considered.

The deformation behavior of the two most representative load cases are shown in Fig. 7A. Under snow load, a maximum vertical deflection of $-156\,\mathrm{mm}$ occurs at point P_1. The base of the pole (P_2) deforms by $-37.9\,\mathrm{mm}$. Under an uplifting wind load, a maximum upward deformation of $119\,\mathrm{mm}$ occurs at point P_1. The base of the pole deforms downward by $-13.9\,\mathrm{mm}$. The largest stress on the top layer occurs under wind loads and the largest stress on the bottom layer occurs under snow loads. Under self-weight and snow (Fig. 7A), the bottom layer is under tension with highest stresses $\sigma_{\mathrm{wire}} = 760\,\mathrm{MPa}$ occurring around the pole. The temperature has a double effect on stress and displacement, during winter the tension increasees whilst displacements decrease, whereas in summer these effects are reversed. The pretension imposed during the erection has a strong effect on the global stiffness which tends to balance the variation induced by the thermal expansion. The pole is used to separate both layers to create a local pretensioning. At the connections with the boundary ring additional tensioning is applied to unify the tension in some critical local areas.

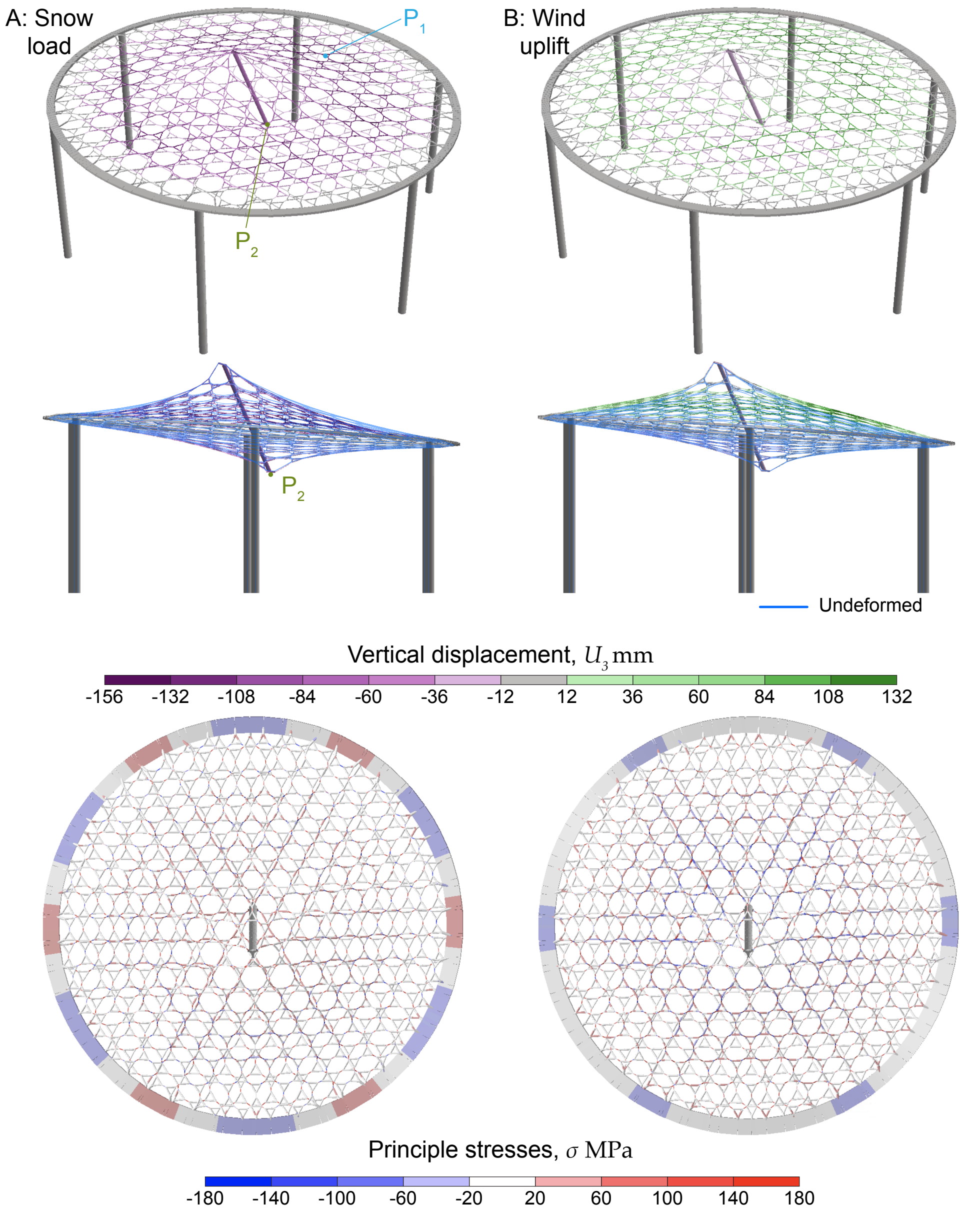

Figure 7: Results of the FE analyses of the simplified beam model. A,B: Displacement and stress plots of load cases for snow, wind uplift, respectively. In the displacement plots, green and purple indicate positive and negative vertical displacement, respectively. In the stress plots, red and blue indicates tension and compression, respectively. The size of triangle and connector elements are magnified 2x for better visibility.

To verify that the beam model can emulate the behavior of the interaction between the panels, the eyelets, and the wire connectors, a volumetric FE simulation is performed on a single panel construction (Fig 8A), where a regular hexagon of edge length 260 mm is modeled with quadratic tetrahedral elements. Both the

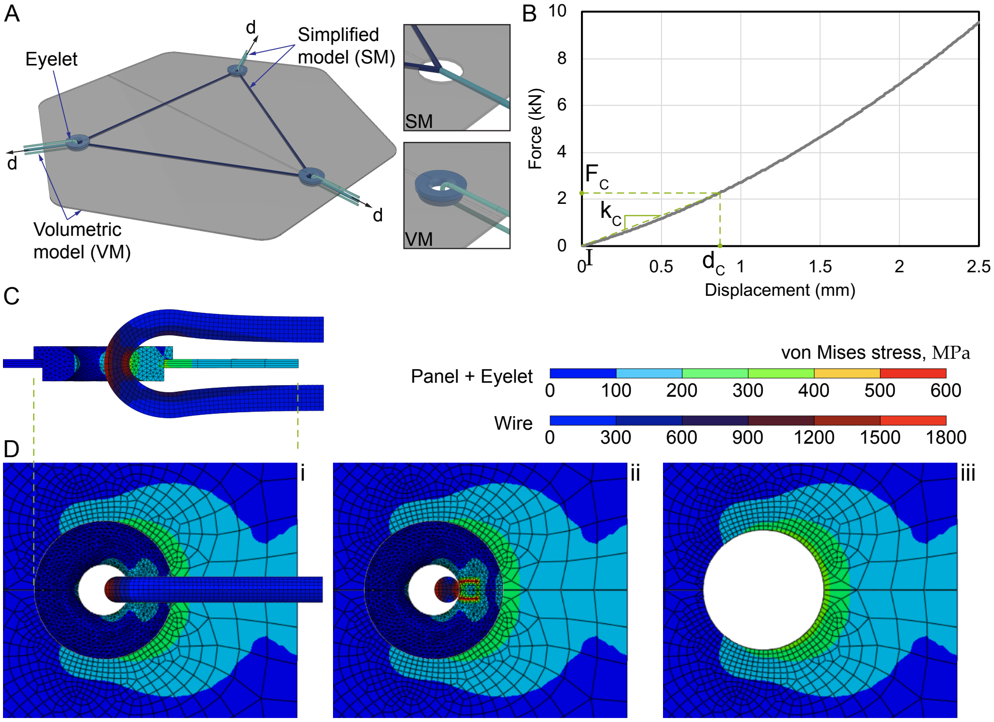

Figure 8: Volumetric FE model of a single hexagonal panel. A: The volumetric and the equivalent beam model. B: The force displacement diagram at the end of the wire connectors. C: Resulting stress plot around the eyelet. D: Top view of the stress plot showing the behavior (i) of the entire construction, (ii) of the eyelet, and (iii) of the panel.

eyelets and the wire connectors are separate geometries that interact with the panel through non-penetrating compressive contacts. It is assumed that the straight wires are able to form a loop connecting neighboring hexagons with negligible stress. The pre-tensioning during erection will ensure that the wires are taut and there is no gap between them and the eyelets. A radial displacement d is applied to each wire end and the corresponding reaction forces are measured. Symmetry conditions are imposed along the $x - z$ plane to reduce computation.

The resulting force displacement diagram (Fig. 8B) shows a gradually stiffening behavior as the wire connector transitions from bending to stretching. An approximate slope of the curve from 0 to the approximate yield of the material is then the effective stiffness of the cable connector k_C. The strength of the wire connector is higher than that of the steel of the eyelet, which is higher than the aluminium panels in turn, i.e. $1570\,\mathrm{MPa} > 660\,\mathrm{MPa} > 310\,\mathrm{MPa}$. These are reached approximately at the same displacement as shown in Fig. 8C,D.

7 Fabrication and Construction

A key benefit of the proposed membrane system is simplicity of fabrication and construction. The hexagonal plates are laser cut from 2 mm aluminium sheet material according to the optimized shape calculated by our algorithm.

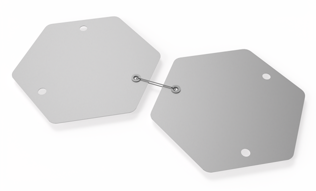

Holes are cut at the vertex locations of the structural triangle embedded in each plate and reinforced with steel eyelets. The wire connector loops are threaded through these eyelets to connect adjacent panels (see inset). Note that while all panels are different, the connectors are all identical, which greatly facilitates assembly.

Each membrane layer is assembled on the ground using labels engraved in the panels to ensure correct positioning. Once connected by the wire loops, the entire layer is lifted onto the circular boundary frame. The top layer is mounted first and temporarily held in place by a crane that fixes the panels linked to the compression pole. The latter is then attached to the top layer and shortened to its minimal length. Subsequently, the lower layer is assembled on the ground in the same manner, lifted onto the boundary ring and connected to the lower end of the compression pole. Variable length connector cables at the boundary ring now allow to deploy the membrane towards its target shape. Finally, the length of the compression pole is adjusted to achieve the desired tensioning in the system. As construction has not yet started at time of printing, please refer to `canopy.epfl.ch` for updates on construction data and photos.

8 Conclusion

The Canopy Pavilion is a first application of deployable auxetics at architectural scale in a permanent building structure. While design and budget constraints did not allow for a more radical exploration of form, our double-membrane structure demonstrates how freeform surfaces can be deployed without any formwork from simple laser cut panels with identical connectors. In this way, the pavilion exemplifies the confluence of geometry, structural optimization, and computational design, linking form and function to digital fabrication and efficient construction.

Acknowledgments

We are grateful to various EPFL entities for generous funding of the Pavilion. This research was supported by the National Centre of Competence in Research (NCCR) Digital Fabrication, funded by the Swiss National Science Foundation (NCCR Digital Fabrication Agreement 51NF40-141853).

References

Bouaziz, S., S. Martin, T. Liu, L. Kavan, and M. Pauly (2014, July). Projective dynamics: Fusing constraint projections for fast simulation. *ACM Trans. Graph. 33*(4), 154:1–154:11.

Deuss, M., A. H. Deleuran, S. Bouaziz, B. Deng, D. Piker, and M. Pauly (2015). *Modelling Behaviour: Design Modelling Symposium 2015*, Chapter ShapeOp—A Robust and Extensible Geometric Modelling Paradigm, pp. 505–515. Cham: Springer International Publishing.

Fornes, M. (2016). Tour de force(s). `https://theverymany.com/public-art/15-harmony-of-the-seas-cruise-ship`. Accessed: 2020-05-12.

Friedrich, J., S. Pfeiffer, and C. Gengnagel (2018). Locally varied auxetic structures for doubly-curved shapes. *Humanizing Digital Reality: Design Modelling Symposium Paris 2017*, 323–336.

Kock, J., B. Bradley, and E. Levelle (2012). Linkage fabric behavior modeling: A case study of chainmail. *Advances in Architectural Geometry*.

Konaković, M., K. Crane, B. Deng, S. Bouaziz, D. Piker, and M. Pauly (2016, July). Beyond developable: Computational design and fabrication with auxetic materials. *ACM Trans. Graph. 35*(4), 89:1–89:11.

Konaković-Luković, M., K. Crane, J. Panetta, and M. Pauly (2018). Rapid deployment of curved surfaces via programmable auxetics. *ACM Trans. Graph.*.

Konaković-Luković, M., P. Konakovic, and M. Pauly (2018). Computational design of deployable auxetic shells. *Advances in Architectural Geometry*.

Mendez Echenagucia, T., D. Pigram, A. Liew, T. Van Mele, and P. Block (2019). A cable-net and fabric formwork system for the construction of concrete shells: Design, fabrication and construction of a full scale prototype. *Structures 18*, 72–82.

Schlaich, J. and R. Bergermann (2004). *leicht weit / Light Structures*. Munich, Germany: Prestel Verlag.